

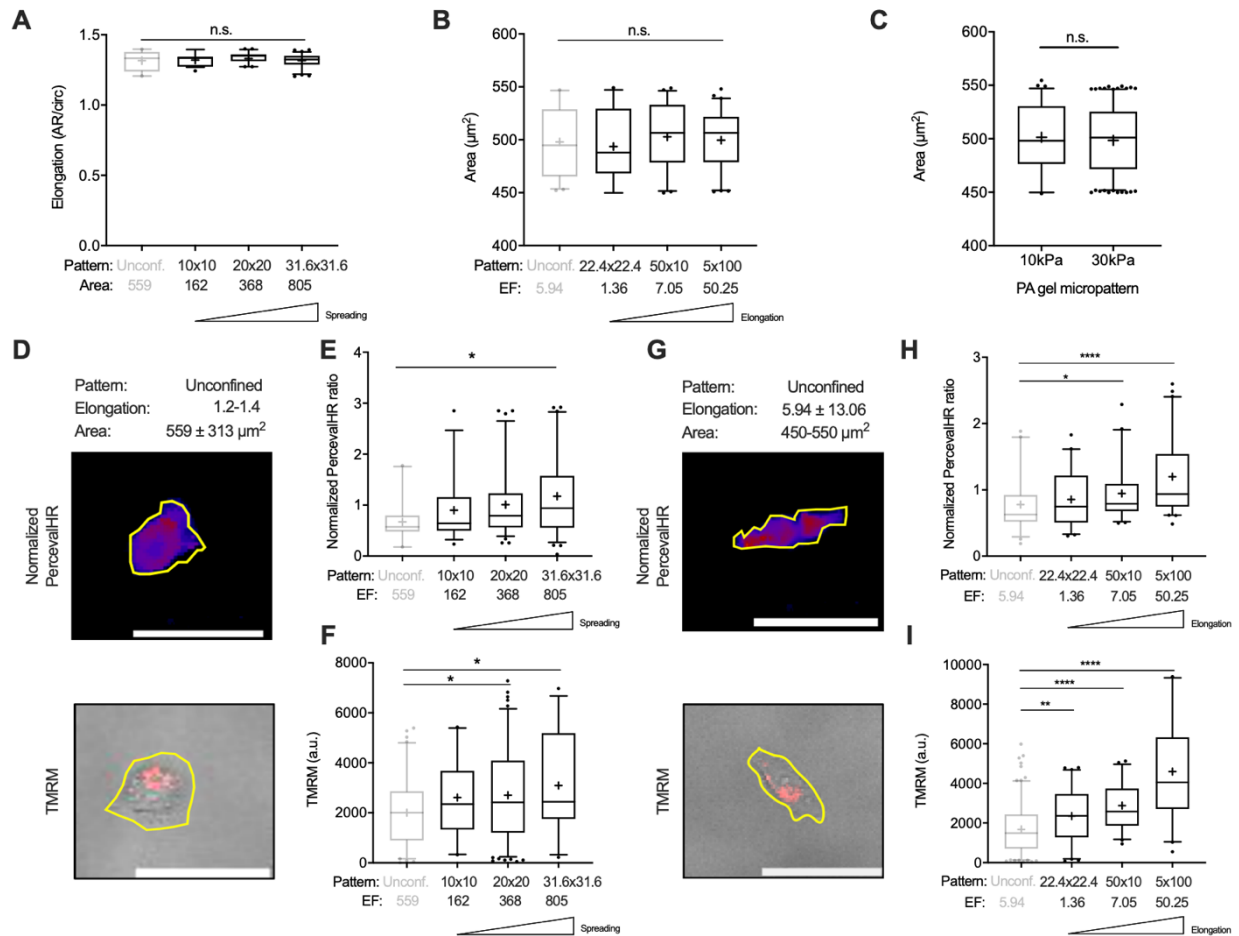
Biophysical Journal, Volume 120

Supplemental information

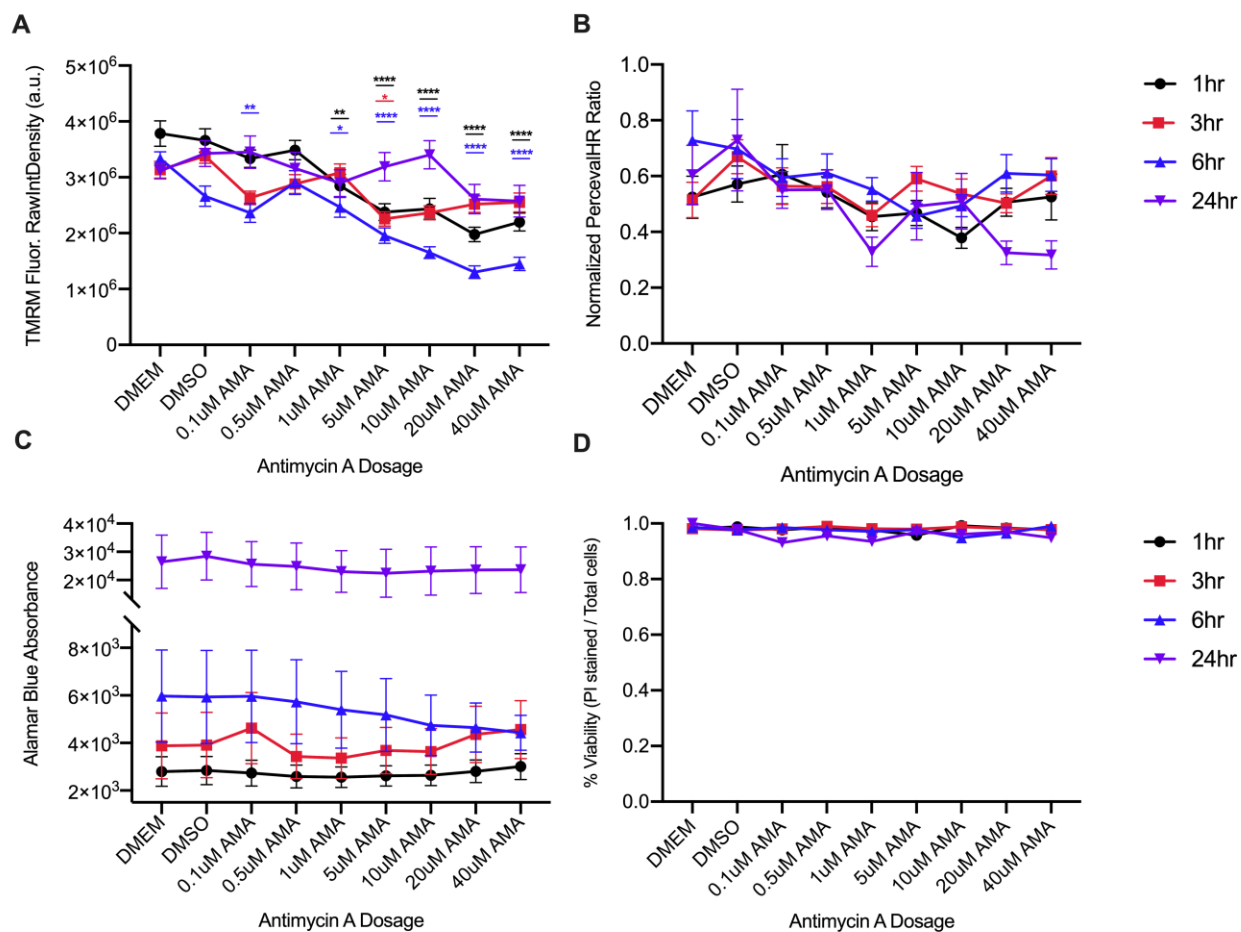
Matrix-driven changes in metabolism support cytoskeletal activity to promote cell migration

Yusheng Wu, Matthew R. Zanutelli, Jian Zhang, and Cynthia A. Reinhart-King

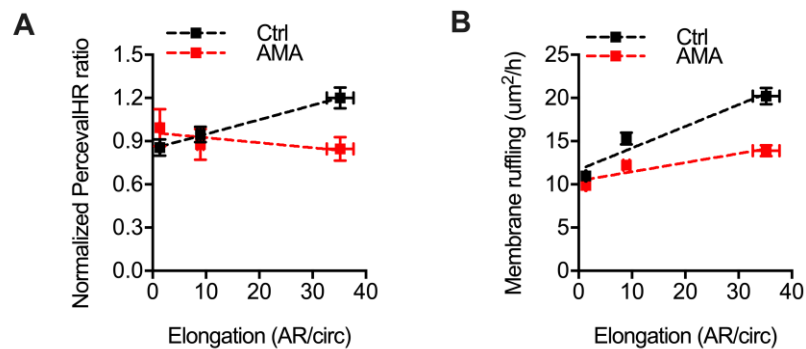
Supplemental figures.



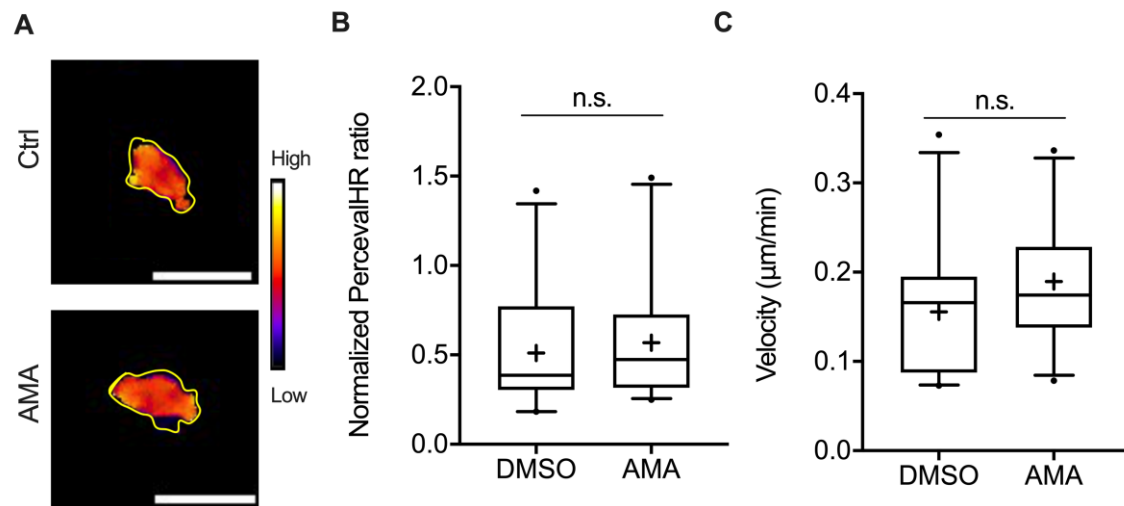
Supplemental Figure 1. Controlling for cell area/elongation and cell confinement across micropattern shapes. Maintaining (A) cell elongation factor across micropattern shape with varying cell area for quantification of MDA-MB-231 PercevalHR signal ($n = 20-76$ cells) and (B) cell area across micropattern shape with varying cell elongation ($n = 50-64$ cells). (C) Maintaining cell area across all micropattern shapes of varying gel stiffness ($n > 100$ cells). (D) Normalized PercevalHR ratio and TMRM fluorescence intensity for MDA-MB-231 cells unconfined on collagen micropatterns. Quantification of (E) normalized PercevalHR ratio ($n = 36-76$ cells) and (F) mitochondrial membrane potential via TMRM ($n = 30-155$ cells) for cells with increasing spreading. (G) Normalized PercevalHR ratio and TMRM fluorescence intensity for MDA-MB-231 cells unconfined on collagen micropatterns. (H) Quantification of normalized PercevalHR ($n = 55-64$ cells) and (I) TMRM for cells with increasing elongation ($n = 40-62$ cells). Data shown as box-and-whisker plots denote mean (+), medians and 25th/75th and 5th/95th percentiles, gray as unconfined and black as patterns; yellow lines show cell outlines. n.s.= non-significant, * $P < 0.05$, ** $P < 0.01$, **** $P < 0.0001$ with one-way ANOVA. Scale bar = 50 μm .



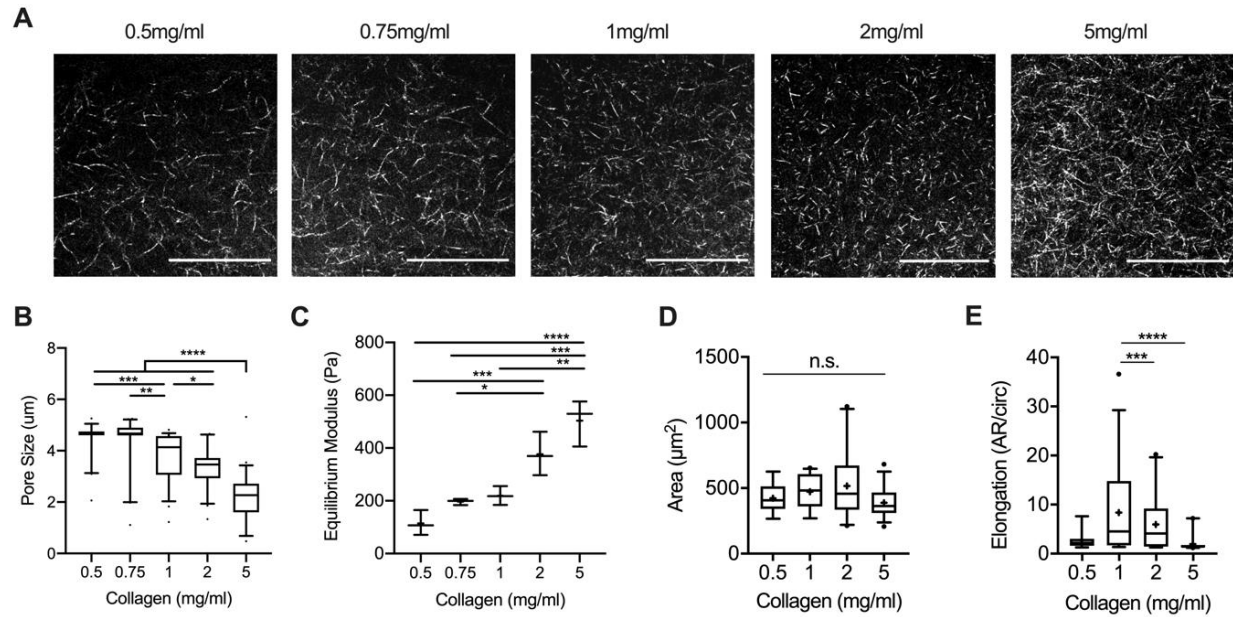
Supplemental Figure 2. OXPPOS inhibition across AMA concentrations. Quantification of (A) mitochondria membrane potential via TMRM integrated fluorescence intensity, (B) normalized PercevalHR ratio, (C) metabolic activity via AlamarBlue fluorescent intensity, and (D) cell viability (propidium iodide (PI) / Hoechst) for 1, 3, 6, and 24 h of treatment with 0.1–40 μ M AMA ($n > 30$ cells). Data shown as mean \pm s.e.m., * $P < 0.05$, ** $P < 0.01$, **** $P < 0.0001$ with one-way ANOVA.



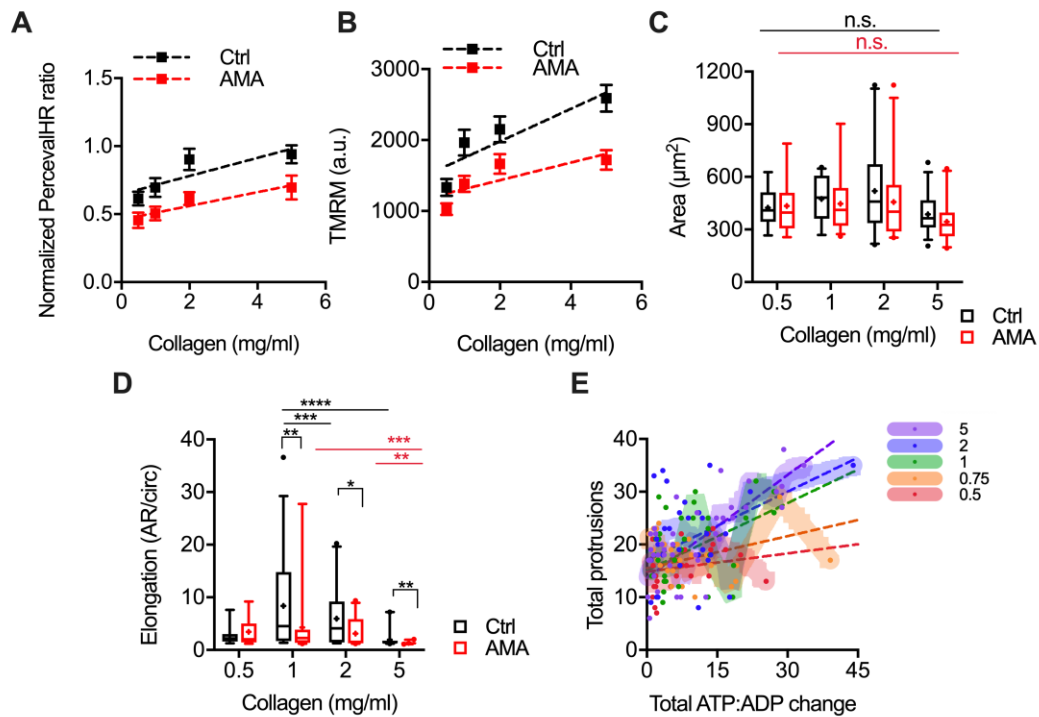
Supplemental Figure 3. OXPPOS impacts intracellular ATP:ADP ratio and membrane ruffling during 2D elongation. (A) Normalized PercevalHR ratio ($n = 55-64$ cells) and (B) membrane ruffling ($n = 30-35$ cells) following AMA treatment on collagen micropatterns with increasing elongation. Data shown as mean \pm s.e.m.; dashed lines show linear regression.



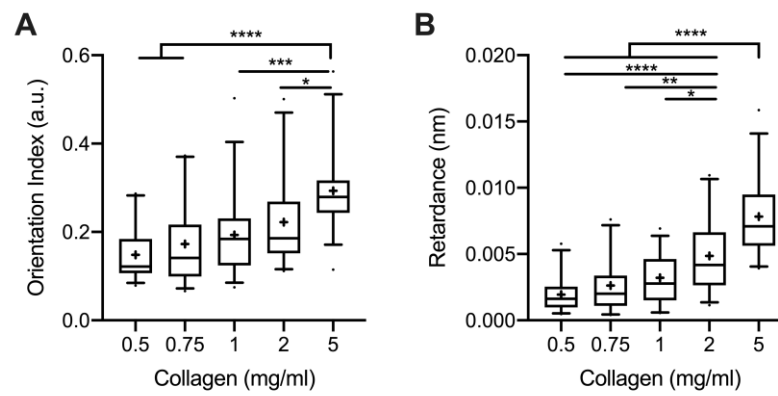
Supplemental Figure 4. OXPPOS inhibition does not influence 2D migration. (A) Normalized PercevalHR ratio of MDA-MB-231 cells following AMA treatment on 2D glass surface. Quantification of (B) Normalized PercevalHR ratio and (C) stepwise velocity after AMA treatment in for 2D migration ($n > 20$ cells). Data shown as box-and-whisker plots denote mean (+), medians and 25th/75th and 5th/95th percentiles; yellow lines show cell outlines; n.s.= not significant with two tailed t-test. Scale bar = 50 μm .



Supplemental Figure 5. MDA-MB-231 cell morphology as a function of 3D collagen density with mechanical characterization. (A) Confocal reflectance images of collagen matrices with varying density. Quantification of (B) pore size and (C) equilibrium modulus of collagen gels with varying density ($n = 3$ gels). Quantification of (D) cell area and (E) cell elongation factor ($n = 16-33$ cells) in matrices with increasing collagen density. Data shown as box-and-whisker plots denote mean (+), medians and 25th/75th and 5th/95th percentiles; multiple comparisons with ANOVA, n.s. = not significant, * $P < 0.05$, ** $P < 0.01$, *** $P < 0.001$, **** $P < 0.0001$. Scale bar = $50 \mu\text{m}$.



Supplemental Figure 6. OXPPOS inhibition impacts morphology and cellular energetics which correlates with protrusions. Linear correlation of collagen density (0.5, 1, 2, and 5mg/ml) with (A) normalized PercevalHR ratio ($n = 32-61$ cells) and (B) TMRM fluorescent signal ($n = 42-93$ cells) following AMA treatment. Quantification of (C) cell area and (D) cell elongation factor ($n = 13-33$ cells) in matrices of increasing collagen densities. (E) Total number of new protrusions and total ATP:ADP change of single MDA-MB-231 cell in collagen matrices ($n = 30-40$ cells). Data shown as box-and-whisker plots denote mean (+), medians and 25th/75th and 5th/95th percentiles, or mean \pm s.e.m.; two-tailed t-test when comparing between ctrl and AMA, multiple comparisons with ANOVA when comparing across densities; lines show LOWESS smoothing and dashed lines show linear regression. n.s. = not significant, ** $P < 0.01$, *** $P < 0.001$, **** $P < 0.0001$.



Supplemental Figure 7. Matrix remodeling and cell contractility increases with collagen density. Quantification of (A) collagen fiber orientation within 10 μ m to cell protrusions and (B) cell contractility for MDA-MB-231 cells in matrices of increasing collagen density. *P < 0.05, **P < 0.01, ***P < 0.001, ****P < 0.0001 with one-way ANOVA.